PCCP

Accepted Manuscript

This is an *Accepted Manuscript*, which has been through the Royal Society of Chemistry peer review process and has been accepted for publication.

Accepted Manuscripts are published online shortly after acceptance, before technical editing, formatting and proof reading. Using this free service, authors can make their results available to the community, in citable form, before we publish the edited article. We will replace this *Accepted Manuscript* with the edited and formatted *Advance Article* as soon as it is available.

You can find more information about *Accepted Manuscripts* in the **Information for Authors**.

Please note that technical editing may introduce minor changes to the text and/or graphics, which may alter content. The journal's standard **Terms & Conditions** and the **Ethical guidelines** still apply. In no event shall the Royal Society of Chemistry be held responsible for any errors or omissions in this *Accepted Manuscript* or any consequences arising from the use of any information it contains.

Dielectric study of insulin-loaded reverse hexagonal (H_II) liquid crystals

T. Mishraki-Berkowitz[a§], P. Ben Ishai[b], A. Aserin[a], Y. Feldman[b] and N. Garti[a*]

Abstract

The dielectric behavior of insulin-loaded H_II mesophase (containing GMO/TAG/water/glycerol/insulin) was studied using two empty reference systems (GMO/TAG/water and GMO/TAG/water/glycerol) at a frequency range of 10^{-2}–10^7 Hz, and temperature range of 290–333 K. Three clearly defined relaxation processes were observed and assigned to the reorientation of GMO polar heads, the tangential movement of counterions at the interface, and the movements of TAGs through the lipid tail. Upon addition of glycerol, a heterogeneous inner structure was formed within the H_II cylinders: water/glycerol core surrounded by water rigid layer. Upon heating, two critical points were detected referring to the dehydration of the GMO heads (at 304 K, similar to the water-filled H_II system) and to energetic modifications (at 316 K), resulting in breaking of the water layer allowing on-demand controlled release. Insulin incorporation combined features of both reference H_II systems. Yet, unlike the empty H_II systems, insulin perturbed the GMO-water interface while decreasing the movement of the GMO headgroup, and reducing T_0 (296 K). No interactions were formed between the dipole of each counterion at the interface region and the matrix (the GMO), fitting Debye process. Dynamic behavior was observed, pointing to mobility between the hexagonal rods themselves, enabling controlled release from the H_II carrier.

Introduction

Reverse hexagonal (H_II) liquid crystals are formed by water and glycerol mono fatty-acid esters (monoglycerides), creating densely packed, long, and straight water-filled rods, arranged within a continuous matrix composed of the fluid lipophilic tails.[1,2] Their two-dimensional symmetry, combined with large interfacial area and their balanced content of hydrophobic and hydrophilic domains produce an applicable matrix for drugs embedment. Due to their unique structure, the H_II mesophases can be used to incorporate drugs within the water core, at the interface or between the lipophilic tails.[3] Of particular interest is the solubilization of therapeutic peptides and proteins.[4] The H_II system based on glycerol monooleate (GMO) was shown to protect the conformational stability of a model protein (lysozyme, LSZ) as a function of the temperature, the pH, and a denaturing agent (urea).[5,6] Additionally, the unique structure of the H_II carriers allows them to be utilized as vehicles for controlled drug delivery, for instance: a hydrophilic peptide (desmopressin) showed lower and better controlled transdermal transport via porcine skin, *in vitro*, when it was embedded within the H_II mesophase, compared to in an aqueous solution.[7] Recently, peptide cell penetration enhancers (CPE) were added to a sodium-diclofenac-loaded H_II mesophase, revealing improved transdermal delivery of the drug through the porcine skin *in vitro*.[8,9] The CPE accelerates the structural transition of skin lipids

from hexagonal to liquid, enhancing diffusion through the *stratum corneum*.[10]

In our previous studies, insulin was incorporated into the H_{II} matrix, provoking disordering of the lipid layer and leading to multiple environments within the interface.[11] Addition of glycerol to the system enhanced the thermal stability of insulin.[12] Yet the dynamic and kinetic properties of the insulin-loaded H_{II} system are still unclear. The understanding of these properties would enable the use of such a valuable vehicle for insulin delivery.

Dielectric spectroscopy (DS) was found to be an efficient method to study the dynamic and kinetic behavior of complex systems, and in particular of the H_{II} mesophase.[13, 14, 15] A complex molecular behavior was detected in and around the interfaces of the GMO-based H_{II} system. Three distinct dielectric relaxations were monitored: the reorientation of GMO polar heads, the tangential movement of counterions at the interface, and the transport of triacylglycerols (triglycerides, TAG) through the lipid tails. One of the main parameters that can be determined using dielectric spectroscopy (DS) is the critical temperature (T_0), which reflects the strength of the intermolecular interactions at the interface, as was demonstrated by phosphatidylcholine (PC) in our previous study.[15] Two processes take place at this critical temperature: (1) the thermal dehydration of the GMO headgroup begins, as was measured by nuclear magnetic resonance (NMR),[16] and (2) the hydrocarbon chain mobility increases, as was shown by EPR.[11] As a result, the hexagonal cylinders shrink, and the lattice parameter decreases, as was detected using SAXS measurements.[16] Additionally, it was found that there is mobility between the H_{II} rods themselves, allowing the incorporated drug to diffuse faster through the matrix.[15]

Accordingly, the goal of the present paper is to study the dielectric properties of insulin-loaded H_{II} mesophase (containing GMO/TAG/water/glycerol/insulin) in order to control its dynamic and kinetic properties for release

purposes. A study of the empty-H_{II} carriers is also included, focusing on the impact of glycerol on the H_{II} matrix, since it not only enhances insulin stability, but also affects the system structure. Glycerol (8 wt%), which has a molecular weight five times greater than water molecules, was added in place of the water. Thus less hydrophilic molecules were located within the cylinders. However, in a homogenous bulk the averaged intermolecular distance (L_m) increases from 3.12 Å for pure water, to 3.50 Å for the current water-glycerol mix.[17] Another possible arrangement to consider is the formation of a heterogeneous structure of the water and glycerol molecules. In addition, since glycerol is hygroscopic, it tends to minimize the area of the lipid-water contact.[18] Although water-glycerol mixtures have been widely studied, confinement of these two solvents cannot predict their dynamics due to two competing effects: (1) surface interactions, which dominate at high temperatures; and (2) geometrical restrictions, which dominate at low temperatures close to T_g.[19,20] Due to the above reasons, the complex water/glycerol-filled H_{II} mesophase should be intensely investigated prior to insulin incorporation.

Results and discussion

The dielectric behavior of the empty H_{II} mesophases (GMO/TAG/water and GMO/TAG/water/glycerol systems), as well as the insulin-loaded H_{II} mesophase (GMO/TAG/water/glycerol/insulin), were measured as a function of frequency (10^{-2}–10^7 Hz) and temperature (290–333 K). For each mesophase, three distinct processes were detected and extensively examined (Fig. 1). The measured data were fit using DATAMA software[21] to the Havrilak–Negami (H-N) phenomenological functions[22] taking into account the *dc* conductivity term:[22]

$$\varepsilon^*(\omega) - \varepsilon_{hf} = \frac{\sigma_{dc}}{i\varepsilon_0\omega} + \sum_{n=1}^{3} \frac{\Delta\varepsilon_n}{\left[1 + \left(i\omega\tau_n\right)^{\alpha_n}\right]^{\beta_n}} \quad (1)$$

where σ_{dc} is the *dc* conductivity, ε_0 is the permittivity of free space, ε_{hf} is the high frequency

2

value of the dielectric permittivity, $\Delta\varepsilon_n$ is the dielectric strength, τ_n is the characteristic relaxation time for the process, and α_n and β_n are parameters ranging from 0 to 1. H-N functions are used to describe complex, frequency-based dielectric data in many complex systems.[23]

Process 1

Process 1, which is ascribed to reorientation of the GMO polar headgroup,[24] was detected in the frequency range of 10^5–10^6 Hz. This reorientation occurs by the breaking of the H-bond at the interface layer of the H_{II} mesophase. The dielectric behavior of the H_{II} systems was fitted using H-N equation (Eq. 1), presenting a Cole-Cole (C-C) process[25] in which β is equal to 1 while α is less than 1. C-C processes are characterized by interaction of the relaxing dipole moment with its underlying physical matrix.[26]

The dielectric permittivity strength ($\Delta\varepsilon$) of the three H_{II} mesophases decreased with temperature (Fig. 2a), confirming that the systems became more fluid. Incorporation of glycerol within the H_{II} mesophase increased $\Delta\varepsilon$ along the entire temperature range compared to the water-filled system. The embedment of insulin within the glycerol-system accentuated this tendency. In the water-filled H_{II} mesophase, the process moved out of the frequency window at 320K, a phenomenon that would probably occur only above the measured temperature range (> 335 K) in the presence of glycerol. The dielectric strength can be interpreted using the following relationship (eq. 2):

$$\Delta\varepsilon \propto g\frac{N\mu^2}{kT} \tag{2}$$

where g is the correlation factor. N is the density of dipoles, μ is the dipole moment, k is the Boltzmann constant, and T is the temperature. The correlation factor, g, indicates the measure of correlation between a reference dipole of the system in question, and the average dipole moment of its neighbors. Should its value be less than 1, then the tendency is to align anti-parallel to the average dipole moment. For g=1 there is no correlation; for g>1 the reference dipole will tend to align itself to the average dipole moment of its neighbors. Since it is less likely that the dipole moment of the GMO heads increases upon addition of glycerol, it is assumed that g and/or N are responsible for the increase of $\Delta\varepsilon$ compared to the water-filled system at a constant temperature. Hence, either the density of GMOs' dipole increased, leading to a more rigid membrane, and/or that the correlation between dipoles increases. For a better understanding of the dielectric behavior, the molecular interactions should be considered. ATR-FTIR results demonstrated that upon addition of glycerol stronger hydrogen-bonds were formed with the GMO headgroups.[12] The relaxation time (τ) supports these findings, demonstrating that the addition of glycerol significantly increased τ (Fig. 2b). Hence, it can be assumed that the dominant process is formation of a rigid membrane as N increases.

It is known that the β-OH group is responsible for the weak binding between heads while the γ-OH is a stronger bond. Thus, the β-OH group would most likely be the first to break. The addition of glycerol probably resulted in "sucking" water away from the interface region around the β-OH site, while simultaneously anchoring the γ-OH. This leads to a stronger interface, but with more GMO head rotation.

The dielectric behavior of water-glycerol solutions was extensively studied as a function of their composition and temperature.[27][28][29][30][31] Water-rich solutions were found to form heterogeneous structures of the liquids. In our case, the molar fraction of glycerol (χ_g) within the H_{II} cylinders is 0.11. At such low concentration, ice nanocrystals surrounded by a water mono-layer (interfacial water) are formed in bulk solution at low temperatures.[27] This value of χ_g was found to be close the minimum point of activation-entropy ($\Delta S^{\ddagger}$) for water/glycerol mixtures (χ_g~0.15).[28] In addition to these energetic considerations, the confinement of

water-glycerol solution can enhance the formation of heterogeneous structures even more, as a result of surface interactions. Elamin et al. proposed that a micro-phase separation occurs in water/glycerol solutions (up to 85 wt% water) confined in a similar pore size (21 Å) conformed by silica matrix MCM-41 with a long chain alkyltrimethylammonium bromide with 10 carbon atoms in the long alkyl group, i.e., $C_{10}H_{21}(CH_3)_3N^+Br$, as the template organic reagent. The micro-phase separation occurs since one of the two liquids has a stronger tendency to coordinate with the hydroxyl groups of the inner pore surface. It was suggested that water molecules are strongly attached to the MCM-41 C10 surface, leaving the glycerol molecules clustered in the center of the pores.[32] Durantini et al. investigated the interactions between different nonaqueous polar solvents and the polar heads of the surfactant in reverse micelles. They concluded that when only glycerol is present, it interacts through hydrogen bonds with the polar heads of the surfactant, thereby removing the counterions from the interface remaining in the polar core of the micelles.[33] However, if that was also the case within the H_{II} mesophase, we would expect an increase in the *dc* conductivity (σ), which is related to the ions located within the cylinder's hydrophilic core. Since, the *dc* conductivity of the two H_{II} mesophases, which was extracted from the fitting function (Eq. 1), were very similar (data not shown), the number of free ions in the bulk was similar. Thus, it can be assumed that a micro-phase separation occurred, forming a secondary interface layer. On their outer side, the water is strongly bonded to the GMO hydroxyls. On their inner side, they interact with a water-glycerol mixture with a higher χ_g.

This unique structure of the water/glycerol core surrounded by two layers of interfaces made by water and GMO heads can be used as a drug encapsulation matrix. It may provide a great advantage for protection of small hydrophilic drugs that will be located at the core and upon heating (at physiological temperature) will release. Such

behavior will provide, on demand, slow and controlled release.

Interesting behavior was detected when insulin was incorporated within the water/glycerol-filled H_{II} matrix. In the presence of insulin $\Delta\varepsilon$ increased and τ decreased (Fig. 2a and b), probably due to the slight weakening of the hydrogen-bonds of the GMO with its surroundings as was detected using ATR-FTIR.[12] To better clarify this behavior, the activation energy (E_α) was extracted using Arrhenius equation:

$$\ln(\tau) = \frac{E_a}{R} \cdot \frac{1}{T} + \ln(A) \quad (3)$$

where R is the gas constant (8.314 J K^{-1}mol^{-1}); T is the temperature; and A is the pre-exponential factor.

In the water-filled H_{II} mesophase, two trends of τ were detected, below and above T_0 (304 K), in which E_α was 33 and 10 KJ/mol, respectively. Addition of glycerol dramatically increased τ and three trends were observed: at 290-304, 304-316, and 316-333 K with E_α of 116, 50, and 68 KJ/mol, respectively. The increase in E_α attests that stronger hydrogen-bonds were formed at the water-GMO interface. Yet, the dehydration-temperature of the GMO headgroups remained intact (T_0 = 304 K). In our previous study we demonstrated how the incorporation of more than 5 wt% of PC within the interface of the H_{II} mesophase increased T_0 as a result of structural modifications. On this basis it can be understood that no major structural alteration occurred at the lipid's interface upon addition of glycerol.[14] The second critical temperature (T_0=316 K) is probably an energetic-process. When the rigid water layer breaks, χ_g decreased as the balance between water/glycerol molecules within the H_{II} core changed. As a result of the decrease of χ_g, the activation-entropy increased, affecting -τ.

Insulin embedment into the water/glycerol-filled H_{II} mesophase decreased T_0 from 304 to 296 K (Fig. 2b), pointing to a structural modification, which characterizes the destabilization of the interface. Three trends were detected at 290-296, 296-320,

and 320-332 K, in which E_α was 93, 21, and 82 KJ/mol, respectively. Insulin probably provoked a disordering of the lipid layer that decreased T_0. These results fit with the EPR study, showing that insulin causes a disordering of the lipid layer, leading to multi-environments within the interface.[11]

The shape parameter, α, in the H-N equation (equation 1) is associated with the dipole-matrix interaction. In our case, the relaxation happening over the matrix can be interpreted as the interaction of the GMO headgroup, rotating by the breaking hydrogen-bonds, with the interfacial layer. Figure 2c presents the behavior of α as a function of τ. The parameter α can be interpreted as a fractal dimension, linking the number density of interactions of the dipole with its matrix, to the various time scales in which this will happen, in essence, a time fractal dimension. It was shown that α can be further related to the spatial fractal dimension of the matrix, D_g, and to the relaxation time, τ, by the relationship:[25]

$$\alpha = \frac{D_g}{2} \frac{\ln(\tau\omega_0)}{\ln(\tau/\tau_0)} \quad (4)$$

where τ_0 is a cut-off timescale for the relaxation process, and ω_0 is a characteristic frequency for the elemental event.

Here, α was examined in two distinct regions – below and above T_0. In the water-filled H_{II} mesophase, D_g is 3.6 below and above T_0. Such phenomenon ($D_g > 3$) characterizes dipole interaction that includes more than one mode of relaxation, a rotation with a translation, because of the additional modes of freedom involved.[14] Below T_0, addition of glycerol to the H_{II} channels did not affect D_g ($D_g = 3.5$). Above T_0, in the temperature range of 304-316 K, D_g drastically dropped, and the relaxation became highly restricted ($D_g = 0.3$), implying formation of a more restricted structure. This may be explained using the increase of N while the H_{II} cylinders shrink upon heating, creating a dense and more restricted environment for

relaxation. In the temperature range of 316-328 K, D_g increased ($D_g = 2.8$), probably as a result of loosening of the water interface, which increases dipole mobility. Above 328 K, D_g dropped to zero as the hexagonal structure started to break.

When insulin was embedded into the H_{II} channels containing water and glycerol, an interesting behavior was detected. Below T_0, the relaxation happened in a layer (D_g=1.1). D_g was lower than in the water and the water/glycerol systems, suggesting that a more restricted structure of the H_{II} cylinders was formed. Apparently, the introduction of insulin at the interface reduced the movement of the GMO headgroups, and as a result D_g dropped. Above T_0, at 296-320 K, D_g decreased to a slight relaxation, heavily restricted (D_g=0.1), showing that the GMO headgroups are strongly held with almost no mobility. Hence, it is assumed that above T_0, insulin entered the interface layer even more, interacting with the GMO carbonyls at the packed cylinders. Above 320 K, D_g can no longer be extracted using equation 4.

Another parameter that can illustrate the relaxation process is N_τ, which is the average number of discrete interactions happening during the time interval $[0,\tau_0]$ in the minimum volume of a sample, which can still be considered as bulk. In our previous publication it was stated that N_τ can be calculated using the following equation:[14]

$$\ln(N_\tau) = \frac{D_g}{2} \ln(\omega_0\tau_0) \quad (5)$$

Below T_0, N_τ refers to the number density of elemental relaxations of the hydrated GMO headgroups. Applying this equation, the calculated N_τ for the water, water/glycerol, and water/glycerol/insulin–filled H_{II} systems were 4.0×10^4, 1.8×10^{12}, and 1.0, respectively. In the water-filled H_{II} system the number of N_τ points to unimpeded relaxation events. The addition of glycerol stabilized the GMO interface, creating even more relaxation events. However, when insulin was incorporated, it dramatically reduced the possibility

of relaxation events of the GMO headgroup. The interface was drastically disordered by the presence of the macromolecule.

Process 2

Process 2, which is recognized as the tangential movement at the interface region of the water's counterions across the GMO headgroup,[34] occurred in the frequency range of 10^2–10^4 Hz. The dielectric behaviors that were fit using the H-N equation also demonstrated C-C process (β=1 in equation 1).

In the water-filled H_{II} mesophase $\Delta\varepsilon$ gradually decreased, confirming that the system became more fluid with temperature (Fig 3a). However, the addition of glycerol presented an opposite trend, in which $\Delta\varepsilon$ increased. This increase can be analyzed using equation 2, determining that the increase in correlation factor, density of dipoles, and/or dipole moment is bigger than the increase of temperature. Since $\Delta\varepsilon$ is based on a virtual dipole of the counterions, it should be explained in terms of transport rather than rigidity. Here again, two critical temperatures were detected, attributed to the thermal and energetic processes. Upon heating, the mobility of the water molecules increased, leading to more available interface for counterion hopping (increase of $\Delta\varepsilon$). The first critical temperature (T_0=304 K) happened as GMO dehydration began. The second critical temperature (320 K) occurred after the rigid water layer broke, decreasing χ_g as the balance between water/glycerol molecules within the H_{II} core changed. As a result of χ_g decrease, the activation-entropy increased, affecting $\Delta\varepsilon$. It should be noted that the quantity of ions (which originate in the water) in the water/glycerol-filled H_{II} system is lower than in the water-filled H_{II} system. Hence, the initial value of $\Delta\varepsilon$ is much lower upon addition of glycerol.

Similarly to an aqua solution, the solubilization of insulin within the H_{II} mesophase is pH dependent. Hence in the insulin-loaded H_{II} mesophase the pH of the water/glycerol was adjusted to 3. In such an acidic environment the high concentration of counterions elevated $\Delta\varepsilon$ by four orders of magnitude. Although the absolute value of $\Delta\varepsilon$ cannot be compared to the empty H_{II} mesophases, the trends of $\Delta\varepsilon$ were examined. $\Delta\varepsilon$ of the insulin-loaded H_{II} system presents a complex behavior with various trends that characterize both the water and the water/glycerol-filled H_{II} systems (Figure 3a). This interesting phenomenon should be analyzed by the structural modifications occurring at the interface. Up to T_0, the GMO headgroups act as in the absence of glycerol, in which $\Delta\varepsilon$ decreased. Insulin (4 wt%), which is located in the core and at the interface, probably prevented the formation of the stable water layer. It creates multi-environments with available surfaces for counterions hopping. At 298-304 K, similarly to the water/glycerol-filled H_{II} system, $\Delta\varepsilon$ drastically increased followed by a gradual decrease. This behavior can be explained in terms of structural modifications as the cylinders shrink, which most likely resulted in an increase of N. Although a secondary water interface was probably not created, it is assumed that the water molecules had stronger tendency to coordinate with the GMO hydroxyl groups, leaving the glycerol molecules clustered in the center of the pores. Figure 3b presents the relaxation time of Process 2 that as expected decreased with temperature. Upon addition of glycerol τ increased. Insulin embedment increased τ even more. Examination of the derivative of τ ($d\tau/dT$) can characterize the model of behavior of the systems. A constant value of τ-derivative points towards Arrhenius behavior (Eq. 3), while deviation from such constancy ($d\tau/dT \neq$ const) indicates Vogel-Fulcher-Tammann (VFT) behavior:

$$\ln(\tau) = \ln(\tau_0) + \frac{F \cdot T_{VFT}}{T - T_{VFT}} \qquad (6)$$

where $0<F^{-1}<1$ is a quantitative measure of fragility and T_{VFT} is the characteristic temperature at which τ diverges.[35][36] VFT is indicative of cooperative processes[37][38] involving cluster coupling, and is especially typical for glass-forming liquids.[39] Since

6

counterion relaxation does not usually obey VFT dynamics, it can be assumed that the cooperative behavior is associated with the GMO tails. The movements of the lipophilic tails indirectly influence the counterions hopping along the interface by the fluctuations they would induce in the GMO heads.[13] T_{VFT} is the ideal temperature at which, in a quasi-static cooling, the system would divest its excess entropy and fall into a crystalline state. This temperature is commonly referred as Kauzmann temperature. The parameter of fragility can quantify how much the system departs from regular Arrhenius dynamics. Bearing in mind the Free Volume approach,[40][41][42][43] F can be defined by a simplified model for the glass transition:

$$F = \frac{f^*}{\alpha_f T_{VFT}} \qquad (7)$$

where f^* is the minimum relative free volume required for the jump of a molecule between two adjacent sites, and α_f is the linear temperature rate of volume expansion. Typical Arrhenius behavior occurs when the available volume of expansion close to the critical temperature ($\alpha_f T_{VFT}$) is smaller than the required volume for relaxation (f^*), hence the fluctuations of the dipole remain local. VFT behavior happens if the available volume of expansion close to the critical temperature is similar to the required volume for relaxation, leading to numerous available configurations for a single relaxation with a strong entropy component. Table 1 summarizes the models of behavior of the three H_{II} systems as a function of T_0.

In the water-filled H_{II} mesophase two different models of behavior were observed. Below T_0, VFT behavior was detected, with $T_{VFT} = 180$ K, $F^{-1} = 0.26$, and $\tau_0 = 1.5 \times 10^{-7}$ s. Above T_0, the system obeyed Arrhenius behavior with $E_\alpha = 14$ KJ/mol (open squares in Figure 3b). These results demonstrate how once the dehydration of the GMO headgroups occurs, the counterions are no longer affected by the motion of the GMO headgroups near them. The addition of glycerol into the system

tremendously modified the system. Below T_0, weak VFT behavior was detected, with $T_{VFT} = 9.6$ K, $F^{-1} = 6.0 \times 10^{-4}$, and $\tau_0 = 1.0 \times 10^{-25}$ s. Above T_0, stronger VFT behavior was detected, with $T_{VFT} = 140$ K, $F^{-1} = 4.9 \times 10^{-2}$, and $\tau_0 = 9.0 \times 10^{-10}$ s (open circles in Figure 3b). These results demonstrate how below T_0, the formation of a stable water layer drastically reduced the mobility of the GMO headgroups. At this point, each counterion was only slightly affected by motion of the GMO headgroup near it. Elevating the temperature increased the mobility and started to destabilize this water layer, resulting in penetration of counterions. Hence, above T_0 the counterions were more affected by the GMO headgroups near them, and stronger VFT behavior was detected.

The incorporation of insulin into the water/glycerol-filled H_{II} system dramatically affected its behavior. It demonstrated Arrhenius behavior below and above T_0, with $E_\alpha = 35$ KJ/mol at 290-296 K and $E_\alpha = -38$ KJ/mol at 298-304 K (solid circles in Figure 3b). The incorporation of insulin disordered the interface and created multi-environments with available surface for counterions hopping, negating the influence of GMO headgroup fluctuation.

To further understand the behavior of the system the nature of the dipole–matrix interaction (α) was examined, representing the relaxation process of the counterion at the interface layer. In contrast to the empty carriers, water and water/glycerol-filled H_{II} systems, in which α is drastically modified with temperature, in the insulin-loaded H_{II} system the value of α was about 1 (Figure 3c). The incorporation of such a macromolecule strongly influenced the dielectric behavior that with good approximation can be fitted to the Debye process (α=1 and β=1 in equation 1). There is almost no interaction between the dipole, which is related to the tangential movement of each counterion at the interface region, and the matrix that is formed by the GMO molecules. The dipole-matrix interactions in the absence of insulin were more complicated, hence the D_g parameter was examined using Eq. (4).

In the water-filled H_{II} mesophase D_g decreased from relaxation in a layer ($D_g = 1.3$) to relaxation in a line ($D_g = 0.2$) due to thermal–structural modification of the hexagonal cylinders. Below T_0, the hydrated GMO headgroups create a relatively strong interface layer that interacts with hopping counterions. Above T_0 the GMO headgroups are dehydrated and are no longer strongly held as a fixed layer. This leads to a decrease of D_g, which implies relaxation in a significantly more fractured environment. An opposite trend was detected upon addition of glycerol. Below T_0, D_g was zero. This means that the water molecules that formed a rigid secondary layer drastically reduced the counterions' mobility along the GMO hydroxyl interface. Above T_0, D_g drastically increased to 4.0, pointing to a full rotation with a translation. Such a high value of D_g indicates that the water secondary layer started to break, allowing the entrance of counterions, leading to free mobility along the interface.

Herein, the parameter N_τ refers to the number of elemental relaxations of the counterions hopping along the hydrated interface during the time interval $[0,\tau_0]$. Applying equation (4), the calculated N_τ for the water and water/glycerol-filled H_{II} systems were 1.0 and 2.8×10^{-2}, respectively. These results can also indicate the structural impact of glycerol incorporation to the water core. Upon addition of glycerol, a secondary layer of water was created, preventing the counterion hopping so their relaxation events were almost impossible to detect.

Process 3

Process 3 is associated with the transport of the TAG molecules through the tails of the GMO, in the frequency range of 0.1–1 Hz.[13] The fittings for this process were done using H-N function, allowing the shape parameters (α and β) to vary from 0 to 2. The dielectric strength of this process is very high (see figure 4) and one could be tempted to assign to Electrode Polarization (EP) processes at the sample/electrode interface. However, the interface is consists of mainly hydrophobic tails and is not conducive to the free motion of ions in this region, a

necessary condition for the building of the Helmholtz layer and consequent electrode polarization.[44] Typically dc conductivity in these systems is in the region of 0.04 Scm^{-1},[13] less than would be expected for a significant EP effect. Therefore one can discount EP as the source of the relaxation.

The fitting parameters cannot describe the dipole reorientation mechanism, but can indicate a percolative system, in which charge transport involves large apparent dipole moments. It had already been shown that the TAG molecule, which possesses a dipole moment of 2 Debye,[45] percolates through the interlacing tails of the GMO.[13] Hence, the data were analyzed using a Laplace transform to the time domain, resulting in the correlation function for the process[46]:

$$\psi(t) = L^{-1}(\varepsilon(\omega)) \qquad (8)$$

where L^{-1} is the inverse Laplace transform operator. The correlation function was fitted using a power and stretch model:[42]

$$\psi(t) = At^{-\mu} \exp[-(t/\tau)^{\nu}] \quad (9)$$

where A is the amplitude, τ is the characteristic relaxation time, and μ and ν are exponents ranging from 0 to 1. This correlation function is associated with transport processes and in particular to percolation.[40] The exponent μ has been related to the growth of cooperative clusters in the system in which charge or excitation transport occurs. The exponent ν is related to transport inside the cooperative cluster. Hence it should be expected that at elevated temperatures the mobility of the continuous phase (the lipophilic region) would increase to form cooperative clusters (larger μ). On the other hand, at elevated temperatures the hexagonal cylinders shrink, leading to less entanglement of the tails in the lipophilic region. Consequently, transport in this region would be more restricted (smaller ν). Yet, a typical percolative system is characterized by a temperature

8

range in which μ reaches a sharp minimum point while ν has a broad maximum point. Such percolated behavior was detected in the water-filled H_{II} system at about 310–325 K (Fig. 4a and b).

In the water-glycerol H_{II} mesophase, μ increased and ν decreased during the whole measured temperature range. Here again T_0 had influenced the process parameters (μ, ν, and τ), presenting moderated trends above T_0 (Fig. 4a-c). This indicates that the dehydration of the interface resulted in increasing the TAG mobility in the lipophilic area. It could be inferred that the formation of the water rigid layer, which strongly bonded to the GMO heads, allowed better transport of TAG molecules along the GMO tails. Thus, percolative behavior should probably be detected only at higher temperatures than the measured range.

Insulin incorporation presents an exceptional behavior. Similarly to the water-filled H_{II} system, typical percolative trend was detected at about 310–325 K (Fig. 4a and b). Yet, unlike the water and the water/glycerol-filled H_{II} systems, τ gradually increased at 300-328 K (Fig. 4c). The increase of τ can indicate that the GMO headgroups were strongly held since insulin penetrated more into the interface layer.

The spatial fractal dimension is followed by the equation:

$$D = 3\nu \qquad (10)$$

The calculated values for the water, water/glycerol, and water/glycerol/insulin-filled H_{II} mesophases are $1.9 < D < 2.0$, $2.1 < D < 2.6$, and $1.8 < D < 2.0$, respectively (Figure 4d). The theoretical value for a static site fractal dimension is 2.53; hence smaller value characterizes a dynamic system.[47] Results reveal that only in the water/glycerol-filled H_{II} system, at 290-292 K, did the hexagonal rods form a stable network of intertwined tails. Yet the mobility of the rods increased with temperature. In both the water and the water/glycerol/insulin-filled H_{II}

mesophases there was mobility between the hexagonal rods themselves at the whole measured temperature range. Rod movements can assist insulin to diffuse faster through the H_{II} carrier. This can be a great advantage in providing controlled release, especially in the case of such a vital protein.

Experimental

Materials

Monoolein, distilled glycerol monooleate (GMO) (min. 97 wt% monoglyceride, 2.5 wt% diglyceride, and 0.4 wt% free glycerol; acid value 1.2, iodine value 68.0, and melting point 37.5ºC) was obtained from Riken Vitamin Co. (Tokyo, Japan). Tricaprylin (triacylglycerol, TAG) (97–98 wt%), glycerol ($\geq$ 99%), and HCl solution (1.0N) were purchased from Sigma Chemical Co. (St. Louis, MO, USA). Insulin human recombinant (28.6 IU/mg) was obtained from Biological Industries (Beit Ha'emek, Israel). The water was double distilled. All ingredients were used without further purification.

Preparation of H_{II} mesophases

Three H_{II} mesophases composed of GMO/TAG/water, GMO/TAG/water/glycerol, and GMO/TAG/water/glycerol/insulin were prepared. In all systems weighed quantities of GMO (72 wt%) and TAG (8 wt%) were mixed while heating to 45°C. This was done in sealed tubes under nitrogen atmosphere to avoid oxidation of the GMO. To the first H_{II} system, 20 wt% water at the same temperature was added. To the second H_{II} system, 12 wt% water and 8 wt% glycerol (water:glycerol with molar ratio of 88.5:11.5) at the same temperature were added. The samples were stirred and cooled to 25°C. In the third H_{II} system, 20 wt% insulin solution, prepared prior to the incorporation into the H_{II} mesophase, was added at 35°C. Insulin solution contained 4 wt% insulin in water:glycerol mixture with weight ratio of 3:2 (molar ratio of 88.5:11.5), and the pH was adjusted to 3.0 with HCl. The sample was stirred at 35°C to avoid the denaturation of the protein and cooled to 25°C.

Dielectric spectroscopy measurements

Dielectric measurements on the H_{II} mesophases were carried out in a frequency range of 0.01 Hz to 1 MHz using a Novocontrol BDS 80 system (Novocontrol GmbH, Hamburg, Germany), based on an Alpha Dielectric Analyzer. Temperature control was provided by a Novocontrol Quatro Cryosystem (Novocontrol GmbH, Hamburg, Germany). The accuracy of measurement in terms of $\tan(\delta)$ is $<10^{-4}$.[48] The samples were mounted between two gold-plated electrode plates with a diameter of 24 mm. Teflon spacers of 1 mm thickness were used to maintain a constant and accurately known distance between the plate electrodes.

Conclusions

The dynamic and the kinetic properties of the complex insulin-loaded H_{II} mesophase (containing GMO/TAG/water/glycerol/insulin) were intensively examined using two empty reference systems, water and water/glycerol-filled H_{II} mesophases. The dielectric behaviors were analyzed at a frequency range of $10^{-2}–10^{7}$ Hz, and temperature range of 290–333 K. Three distinct processes were monitored: (1) the reorientation of GMO polar heads, (2) the tangential movement of counterions at the interface, and (3) the shift of TAGs through the lipid tails.

The present study demonstrates how addition of glycerol (χ_g=0.11) to the water core formed a heterogeneous structure within the H_{II} cylinders. A rigid water layer was produced, which strongly

bonded to GMO heads and even created a static system (no mobility between hexagonal rods) at 290–292 K. Two critical temperatures were detected at 304 and 316 K, pointing to dehydration of the GMO heads and energetic modifications that resulted in breaking of the water interface layer, respectively. This unique structural behavior is especially advantageous for encapsulation of small hydrophilic drugs, by providing them "on demand" and with controlled release.

Incorporation of insulin into the water/glycerol-filled H_{II} mesophase presented exclusive behavior, combining characteristics of the both reference H_{II} systems. Since insulin is a macromolecule it perturbed the interface (which probably prevented the formation of the water rigid layer), resulting in both reduction of the movement of the GMO headgroup, and decreased T_0 (296 K). Unlike the empty H_{II} mesophases, there was almost no interaction between the dipole of the tangential movement of each counterion at the interface region, and the matrix (the GMO) fitting the Debye process. Similarly to the water-filled H_{II} mesophases, the system was dynamic, i.e., there was mobility between the hexagonal rods themselves. This mobility might be advantageous for insulin release from the H_{II} carrier.

Notes and references

[a] The Ratner Chair in Chemistry, Casali Institute of Applied Chemistry, The Institute of Chemistry, The Hebrew University of Jerusalem, Edmond J. Safra Campus, Jerusalem 91904, Israel.

[b] Department of Applied Physics, The Hebrew University of Jerusalem, Edmond J. Safra Campus, Jerusalem 91904, Israel.

[§]The results presented in this paper will appear in the Ph.D. dissertation of T.M.B. in partial fulfillment of the requirements for the Ph.D. degree in Applied Chemistry, The Hebrew University of Jerusalem, Israel.

*Author to whom correspondence should be addressed

Tel: +972-2-658-6574/5

Fax: +972-2-652-0262

E-mail: garti@vms.huji.ac.il

[1] G. J. T. Tiddy, *Physics Reports – Review Section of Physics Letters,* 1980, **57**, 2–46.

[2] J. M. Seddon, *Biochem. Biophys. Acta,* 1990, **1031**, 1–69.

[3] C. Guo, J. Wang, F. Cao, R. J. Lee, G. Zhai, *Drug Discov. Today,* 2010, **15**, 1032-1040.

[4] D. Libster, A. Aserin, N. Garti, *J. Coll. Interface Sci*., 2011, **356**, 375–386.

[5] T. Mishraki, D. Libster, A. Aserin, N. Garti, *Colloids Surf. B,* 2010, **75**, 47–56.

[6] T. Mishraki, D. Libster, A. Aserin, N. Garti, *Colloids Surf. B,* 2010, **75**, 391–397.

[7] D. Libster, A. Aserin, D. Yariv, G. Shoham, N. Garti *Colloids Surf. B,* 2009, **74**, 202–215.

[8] M. Cohen-Avrahami, A. Aserin, N. Garti, *Colloids Surf. B,* 2010, **77**, 131–138.

[9] M. Cohen-Avrahami, D. Libster, A. Aserin, N. Garti, *J. Phys. Chem. B,* 2011, **115**, 10189–10197.

[10] M. Cohen-Avrahami, D. Libster, A. Aserin, N. Garti, *J. Control. Release,* 2012, **159**, 419–428.

[11] T. Mishraki, M. F. Ottaviani, A. I. Shames, A. Aserin, N. Garti, *J. Phys. Chem. B,* 2011, **115**, 8054-8062.

[12] I. Amar-Yuli, D. Azulay, T. Mishraki, A. Aserin, N. Garti, *J. Coll. Interface Sci.,* 2011, **364**, 379–387.

[13] P. Ben Ishai, D. Libster, A. Aserin, N. Garti, Y. Feldman, *J. Phys. Chem. B* 113 (2009) 12639–12647.

[14] P. Ben Ishai, D. Libster, A. Aserin, N. Garti, Y. Feldman, *J. Phys. Chem. B,* 2010, **114**, 12785–12791.

[15] T. Mishraki, P. Ben Ishai, D. Babukh, A. Aserin, Y. Feldman, N. Garti, *J. Coll. Interface Sci.,* 2013, **396**, 178–186.

[16] I. Amar-Yuli, E. Wachtel, D. E. Shalev, H. Moshe, A. Aserin, N. Garti, *J. Phys. Chem. B,* 2007, **111**, 13544–13553.

[17] A. Puzenko, Y. Hayashi, Y. Feldman, *J. Non-Cryst. Sol.,* 2007, **353**, 4518–4522.

[18] R. Koynova, J. Brankov, B. Tenchov, *Eur. Biophys. J.,* 1997, **25**, 261–274.

[19] M. Alcoutlabi, G. B. McKenna, *J. Phys.: Condens. Matter,* 2005, **17**, R461–R524.

[20] P. Pissis, A. Kyritsisy, D. Daoukakiy, G. Barutz, R. Pelsterz, G. Nimtzz, *J. Phys.: Condens. Matter,* 1998, **10**, 6205–6227.

[21] N. Axelrod, E. Axelriod, A. Gutina, A. Puzenko, P. Ben Ishai, Y. Feldman, *Sci. Technol.,* 2004, **15**, 755–764.

[22] S. Havriliak, S. Negami, *J. Polym. Sci. Part C,* 1966, **14**, 99–117.

[23] C. J. F. Bottcher, Theory of electric polarization: Dielectrics in time-dependent fields. 2nd ed. Elsevier Science Ltd.: Amsterdam, The Netherlands, New York, 1980.

[24] G. E. Crawford, J. C. Earnshaw, *Biophys. J.,* 1987, **52**, 87–94.

[25] K. S. Cole, R. H. Cole, *J. Chem. Phys.,* 1941, **9**, 341–351.

[26] Y. Ryabov, Y. Feldman, *Physica A.,* 2002, **314**, 370–378.

[27] A. Puzenko, Y. Hayashi, Y. E. Ryabov, I. Balin, Y. Feldman, U. Kaatze, R. Behrends, *J. Phys. Chem. B,* 2005, **109**, 6031-6035.

[28] Y. Hayashi, A. Puzenko, I. Balin, Y. E. Ryabov, Y. Feldman, *J. Phys. Chem. B,* 2005, **109**, 9174–9177.

[29] Y. Hayashi, A. Puzenko, Y. Feldman, *J. Phys. Chem. B,* 2005, **109**, 16979–16981.

[30] Y. Hayashi, A. Puzenko, Y. Feldman, *J. Non-Cryst. Sol.,* 2006, **352**, 4696–4703.

[31] R. Behrends, K. Fuchs, U. Kaatze, Y. Hayashi, Y. Feldman, *J. Chem. Phys.,* 2006, **124**, 144512 –144518.

[32] K. Elamin, H. Jansson, S. Kittaka, J. Swenson, *Phys. Chem. Chem. Phys.,* 2013, **15**, 18437–18444.

[33] A. M. Durantini, R. D. Falcone, J. J. Silber, N. M. Correa, *Chem. Phys. Chem.,* 2009, **10**, 2034–2040.

[34] I. Ermolina, G. Smith, Y. Ryabov, A. Puzenko, Y. Polevaya, R. Nigmatullin, Y. Feldman, *J. Phys. Chem. B,* 2000, **104**, 1373–1381.

[35] C. A. Angell, in: M. Rubi, C. Perez-Vicente (Eds.), vol. 492, Springer Berlin Heidelberg, 1997, pp. 1–21.

[36] C. A. Angell, *J. Non-Cryst. Sol.,* 1991, **131**, 13–31.

[37] C.A. Angell, *Science,* 1995, **267**, 1924–1935.

[38] J. Green, K. Ito, K. Xu, C. Angell, *J. Phys. Chem. B,* 1999, **103**, 3991–3996.

[39] Y. Feldman, A. Puzenko, Y. Ryabov, in: W. T. Coffey, Y .P. Kalmykov (Eds.), Fractals, Diffusion and Relaxation in Disordered Complex Systems: Advances in Chemical Physics, Part A, vol. 133. John Wiley & Sons, 2006, pp. 1–125.

[40] J. Green, K. Ito, K. Xu, C. Angell, *J. Phys. Chem. B,* 1999, **103**, 3991–3996.

[41] M. H. Cohen, G. S. Grest, *Phys. Rev. B,* 1979, **20**, 1077–1098.

[42] M. H. Cohen, D. Turnbull, *J. Chem. Phys.,* 1959, **31,** 1164–1169.

[43] A. K. Doolittle, *J. Appl. Phys.,* 1951, **22**, 1471–1475.

[44] P. Ben Ishai, M. S. Talary, A. Caduff, E. Levy, Y. Feldman, Meas. Sci. Technol. 2013, **24,** 102001-21.

[45] T. Ivanova, K. Mircheva, G. Dobreva, I. Panaiotov, J. Proust, R. Verger, *Colloid. Surf. B,* 2008, **63**, 91–100.

[46] A. K. Jonscher, Universal Relaxation Law, Chelsea Dielectrics Press, London, 1996.

[47] Y. Feldman, A. Puzenko, Y. Ryabov, *Chem. Phys.,* 2002, **284**, 139–168.

[48] User's Manual, 2000. Alpha high resolution dielectric analyser.

Figure legends

Figure 1: The monitored dielectric permittivity (ε') of (□) water-filled H_{II} mesophase, (○) water/glycerol-filled H_{II} mesophase, and (●) water/glycerol/insulin-filled H_{II} mesophase; at 290 K.

Figure 2: (a) The dielectric strength ($\Delta\varepsilon$) as a function of temperature, (b) the characteristic relaxation time as a function of inverse temperature, and (c) the stretch parameter (α) as a function of relaxation time (τ), for Process 1. H_{II} mesophases are composed of (□) water-filled H_{II} mesophase, (○) water/glycerol-filled H_{II} mesophase, and (●) water/glycerol/insulin-filled H_{II} mesophase.

Figure 3: (a) The dielectric strength ($\Delta\varepsilon$) as a function of temperature, (b) the characteristic relaxation time as a function of inverse temperature, and (c) the stretch parameter (α) as a function of temperature, for Process 2. H_{II} mesophases are composed of (□) water-filled H_{II} mesophase, (○) water/glycerol-filled H_{II} mesophase, and (●) water/glycerol/insulin-filled H_{II} mesophase.

Figure 4: (a) The power parameter (μ), (b) the stretch parameter (ν), (c) the relaxation time, and (d) the spatial fractal dimension as a function of temperature of (□) water-filled H_{II} mesophase, (○) water/glycerol-filled H_{II} mesophase, and (●) water/glycerol/insulin-filled H_{II} mesophase, for Process 3.
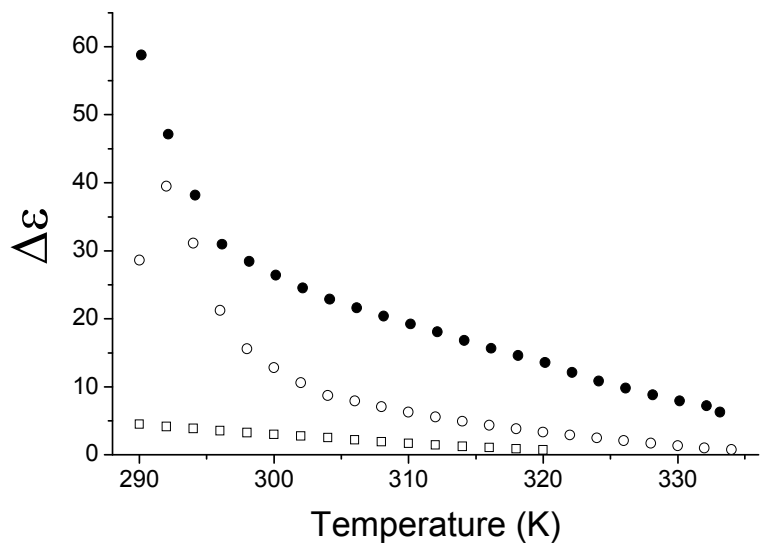
Table caption

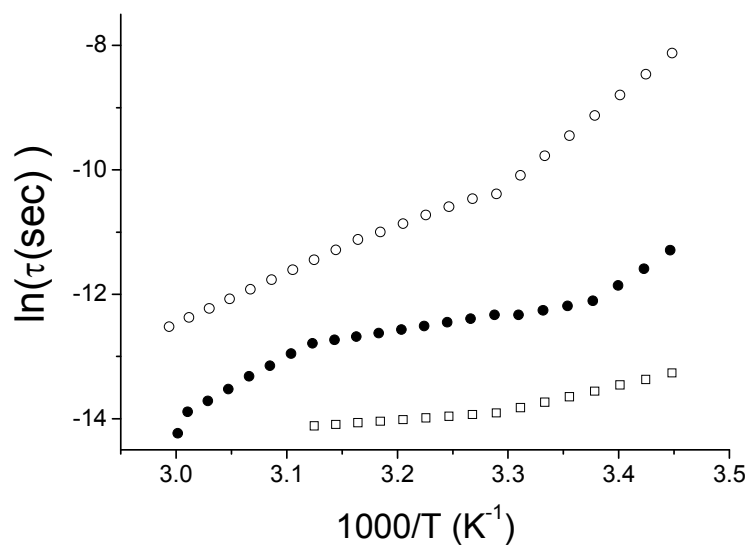Table 1: The models of behavior of the different H_{II} systems as a function of T_0, in Process 2.
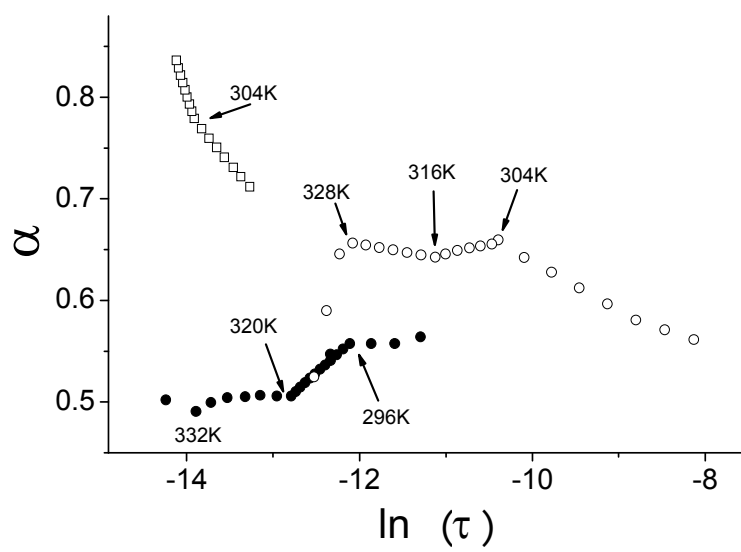
1.
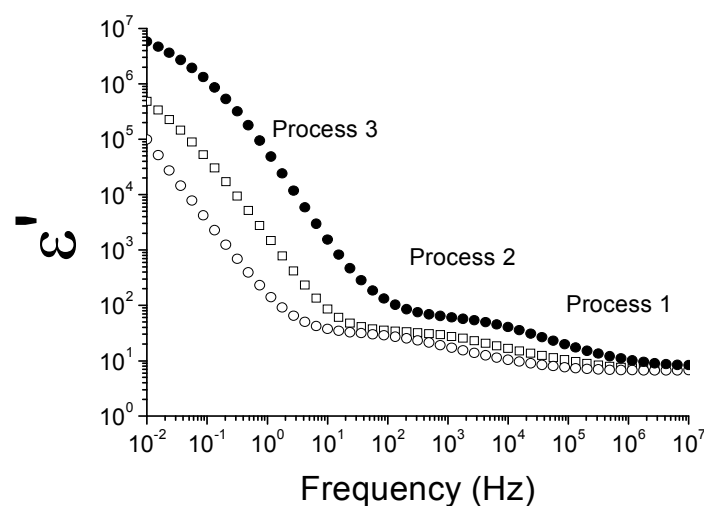
2. (a)

(b)

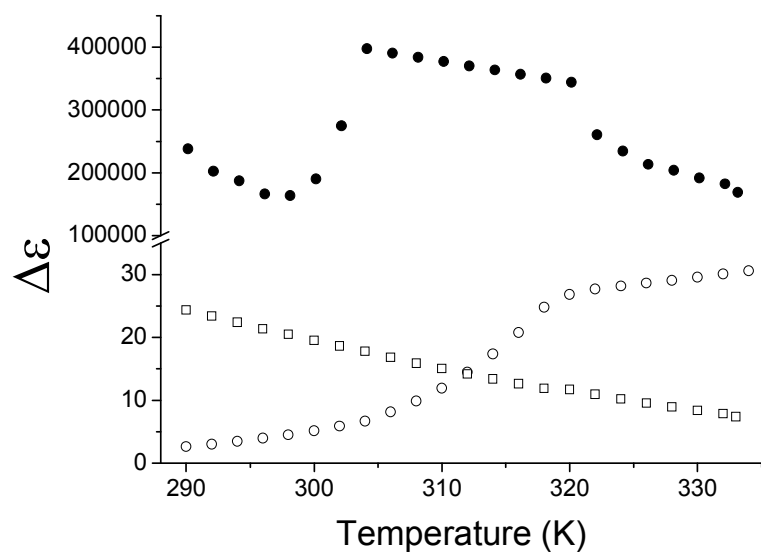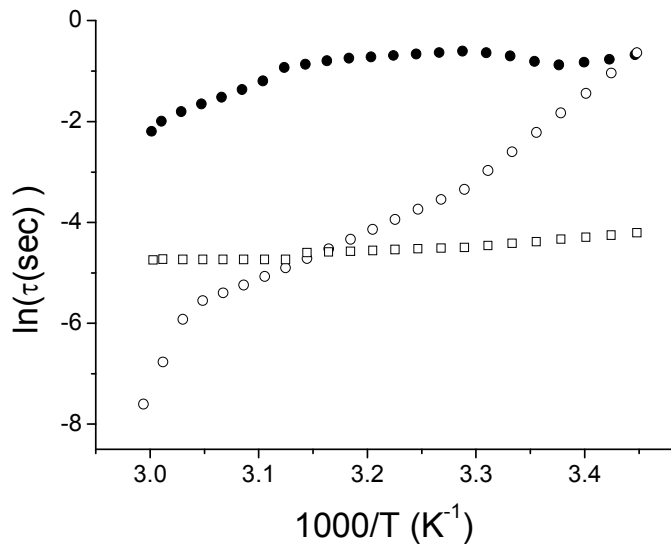(c)

3.

(a)

(b)

(c)
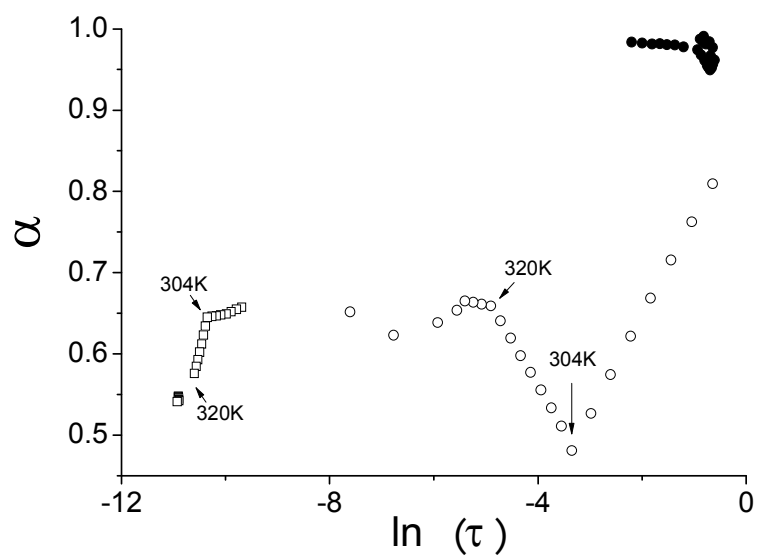
4. (a)
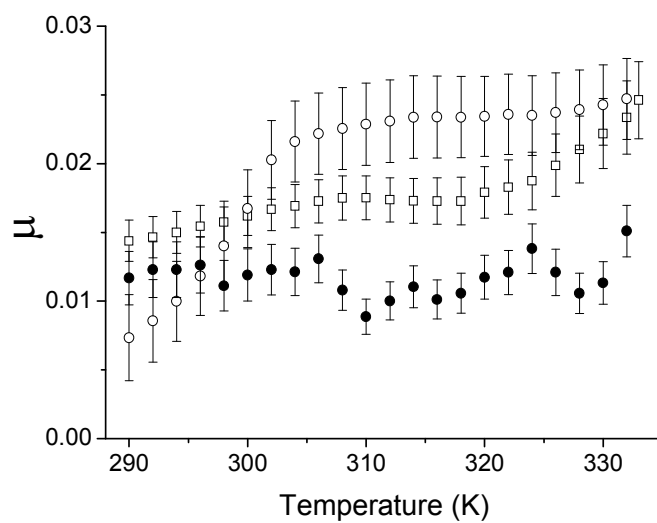
(b)
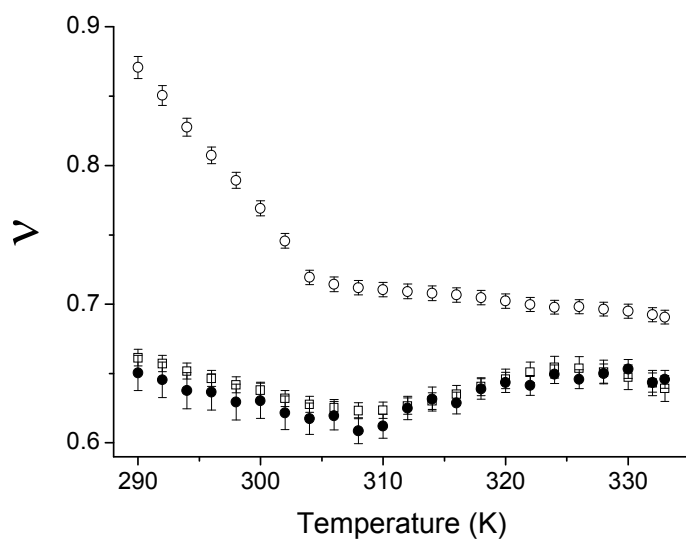
(c)

(d)

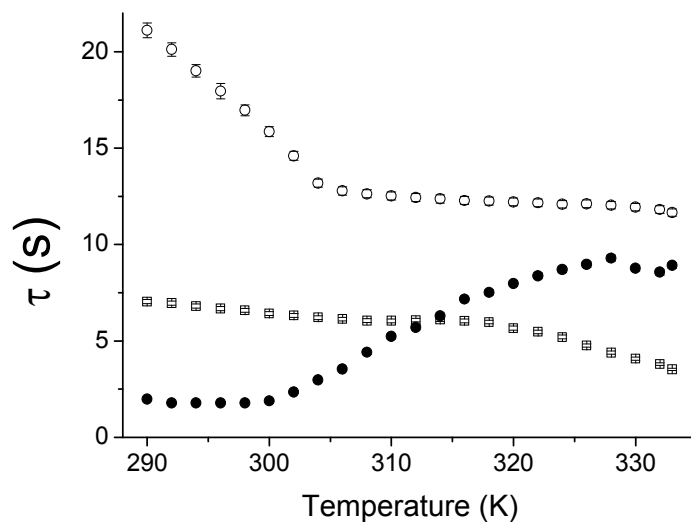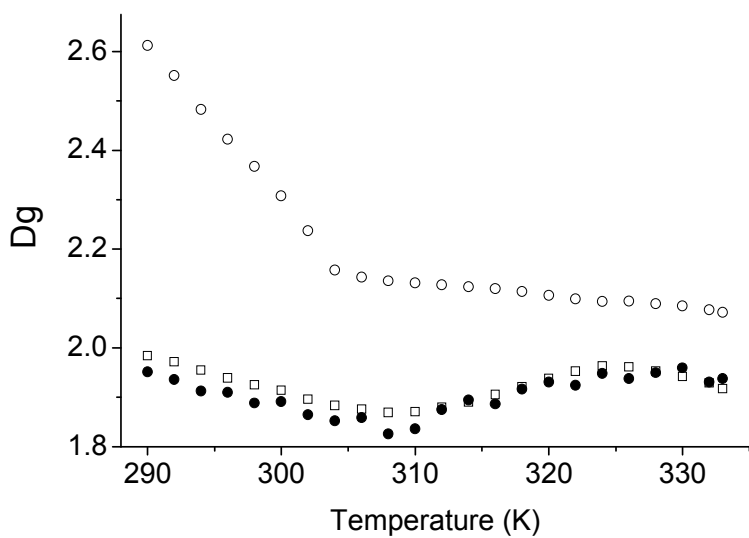|	$T < T_0$	$T > T_0$
GMO/TAG/water	VFT	Arrhenius
GMO/TAG/water/glycerol	VFT	VFT
GMO/TAG/water/glycerol/insulin	Arrhenius	Arrhenius

18